RSC Advances

PAPER

View Article Online
View Journal | View Issue

Cite this: *RSC Adv.*, 2024, **14**, 32389

To treat wastewater with wastes: a highly efficient flocculant from fly ash and rice straw†

Shuichang Chen,[ab] Shiqian Li,[*b] Wanghua Wu,[ab] Haodong Ye,[c] Haiqing Liu,[a] Shibin Ma[d] and Qinghua Chen[*a]

Received 31st July 2024
Accepted 12th September 2024

DOI: 10.1039/d4ra05550k

rsc.li/rsc-advances

Water resources are vital for sustainable human life and economic activities. However, the issue of water pollution has reached alarming levels. Coking wastewater, known for its high concentrations of organic matter and toxic substances, poses significant environmental hazards. In response to this challenge, we developed a novel composite flocculant called polymeric aluminum ferric chloride (PAFC)/rice straw (PAFC/RS) from fly ash (a coal waste) and rice straw (an agricultural waste). The PAFC/RS was characterized by X-ray powder diffraction (XRD), scanning electron microscopy (SEM) and Fourier transformed infrared (FT-IR). The flocculation performance of PAFC/RS was studied utilizing humic acid simulated coking wastewater as the target by measuring the chemical oxygen demand (COD), UV_{254}, and turbidity. A removal efficiency of 97.3% for turbidity, 79.7% for COD, and 98.2% for UV_{254} was reached for the PAFC/RS with an optimal composition. It demonstrated a better flocculation effect compared to the traditional aluminum–iron-based inorganic flocculant. The PAFC/RS possesses great potential for a straightforward, cost-effective, and environmentally friendly water treatment material.

1. Introduction

Coking wastewater from coal industry operations, is notorious for its complex compositions including a myriad of organic and inorganic pollutants, posing substantial risks to human health.[1] Chemical oxidation has traditionally been utilized for coking wastewater treatment, but it is costly and frequently yields a substantial residue of pollutants,[2] requiring further treatments. Another prevalent approach involves biochemical treatment for its efficacy in mitigating a considerable portion of organic pollutants.[3] However, biochemical treatment frequently encounters challenges in degrading recalcitrant humic organic pollutants. This approach yields a biochemical effluent with COD levels soaring as high as 300 mg L^{-1}, especially when the wastewater contains elevated concentrations of recalcitrant COD compounds.[4] Therefore, this has spurred the adoption of flocculants due to their straightforward application and efficient removal of pollutants from secondary biochemical effluents, thus emerging as the predominant treatment approach.[5] Numerous popular flocculants exist, primarily including inorganic flocculants, synthetic and natural polymer flocculants, and composite flocculants.[6]

Common inorganic flocculants primarily include aluminum-based and iron-based compounds, such as alum, aluminum chloride, polymerized aluminum silicate, polymerized aluminum chloride, and polymerized aluminum ferric chloride (PAFC). Inorganic flocculants exhibit effective flocculation and are simple to prepare. However, their flocculation can be incomplete, and some may even leave high metal residues. Synthetic polymer flocculants, such as polyacrylamide-based ones, have high flocculating capacity, but their environmental impact is controversial.[7] Consequently, there is a significant interest in developing natural polymer flocculants using readily available, cost-effective polysaccharides to enhance biodegradability. However, natural polymer flocculants face challenges, including insufficient flocculation efficiency and the need for large quantities.[8] Consequently, researchers have focused on developing inorganic/organic polymeric composite flocculants. However, the composite flocculants composed of inorganic flocculants and biomass polymers remain limited.

Effective flocculation can be achieved by combining natural polymeric materials with inorganic flocculants through grafting or physical mixing.[9] Recently, natural organic materials such as starch, sodium alginate, chitosan, and cellulose have seen widespread use to enhance the environmental compatibility of organic and inorganic flocculants. Cellulose harbors a plenty of hydroxyl groups. Surface functionalization of cellulose *via* physical or chemical means can markedly augment its flocculation efficiency. Straw, rich in hemicellulose and wax,

[a]*College of Chemistry and Materials Science, Fujian Normal University, Fuzhou 350117, China. E-mail: cqhuar@126.com*

[b]*College of Materials and Package Engineering, Fujian Provincial Key Lab of Coastal Basin Environment, Fujian Polytechnic Normal University, Fuqing 350300, China. E-mail: lishiqian@whu.edu.cn*

[c]*College of Agriculture, Guangxi University, Guangxi 530004, China*

[d]*Fujian Rongqi Constuction Engineering Co., Ltd, Fuqing 350300, China*

† Electronic supplementary information (ESI) available. See DOI: https://doi.org/10.1039/d4ra05550k

undergoes alkali treatment to remove these constituents.[10,11] This process leads to the formation of irregular crevices and even a reticulate structure on the originally smooth surface of the straw, while maintaining its initial fiber structure.[12,13] Combining polymeric aluminum ferric chloride with treated straw is a potential method for preparing efficient composite flocculants.

Herein, we made an inorganic/organic composite flocculant of PAFC/straw (PAFC/RS) from coal and agricultural wastes of fly ash and rice straw. Its structure was characterization using XRD, FTIR, and SEM techniques. Its removal efficiency of the humic acid in a simulated coking wastewater was evaluated. We found that it can effectively mitigate this pollutant in the wastewater. From the viewpoints of cost and efficiency, PAFC/RS presents a highly promising flocculant for the treatment of the coking water.

2. Materials and methods

2.1. Materials

Fly ash was provided by Gongyi Hengnuo Filter Media Co., China (include 35% silicon dioxide, 8% iron oxide, 27% aluminum oxide, 15% calcium oxide, and small amounts of magnesium oxide, potassium oxide, and sodium oxide). Hydrochloric acid and sulfuric acid were purchased from Sinopharm Chemical Reagent Co., China. Sodium hydroxide was purchased from Xilong Science Co., China. Kaolin and potassium dichromate were purchased from Tianjin Damao Chemical Reagent Factory, China. Ferrous ammonium sulfate was purchased from Tianjin Beichen Fangzheng Reagent Co., China. Commercial PAFC (cPAFC) was purchased from Nanjing Yuanling Chemical Co., China. Mercury sulfate was purchased from Guizhou Tongren Chemical Reagent Factory, China. Silver sulfate was purchased from Wuhan Elirier High tech Co., China. Humic acid (HA) and ferrous indicator were purchased from Shanghai Aladdin Biochemical Co. The raw rice straw (RS) was collected from a farmland in Fuzhou City, Fujian Province, China. It was washed three times with deionized water and dried in a 105 °C oven for 24 h. The dried straw was ground and sieved through an 80 mesh sieve to obtain rice straw powders. Subsequently, they were treated in 10 wt% NaOH aqueous solution at a liquid-to-solid ratio of 1/20 (L g^{-1}) for 24 h at 25 °C. Then the precipitates were collected after centrifugation, followed by washing with deionized water until the supernatant reaches neutral. Finally, they were dried at 80 °C for 72 h and named as RS-10 used for the following studies.

2.2. Preparation of PAFC/RS

The fly ash was treated in 10 wt% HCl aq. solution in a liquid-to-solid ratio of 3/1000 (L g^{-1}) at 70 °C for 3 h under the condition of condensation reflux. The supernatant was collected by centrifugation (the primary components of fly ash leachate are aluminum chloride, iron chloride, calcium chloride, and small amounts of potassium chloride, magnesium chloride, and sodium chloride). Its pH was adjusted to 4 by addition of 10 wt% NaOH solution. Into it, a certain amount of RS-10 was subsequently added and stirred at 200 rpm at 70 °C for 1 h, then let it stand at this temperature for 2 h. The supernatant was removed, and the lower layer is precipitated in the oven at 70 °C for 12 h and then ground to obtain PAFC/RS-10 composite powder. Polymerized aluminum ferric chloride (PAFC) was prepared under the same conditions. The products obtained are designated as PAFC-A/RS-B, where A represents the mass-to-volume ratio of RS to the acid leaching solution (g L^{-1}), and B indicates the mass concentration of NaOH aq. solution used in the straw treatment. For instance, samples prepared by adding RS-10 to the acid leaching solution at ratios of 5 g L^{-1}, 10 g L^{-1}, 15 g L^{-1}, 20 g L^{-1}, and 25 g L^{-1} were named PAFC-5/RS-10, PAFC-10/RS-10, PAFC-15/RS-10, PAFC-20/RS-10, and PAFC-25/RS-10, respectively. The preparation procedure of PAFC/RS is shown in Fig. 1. During the reaction, the hydrolysis products of aluminum and iron interact, forming a high molecular weight mixture containing polynuclear hydroxyl complexes. PAFC is immobilized on the RS surface *via* hydrogen bonding between the hydroxyl groups in the polynuclear hydroxyl complex and those on the straw. The reaction formula of PAFC polymerization process is as shown in eqn (1)–(3).

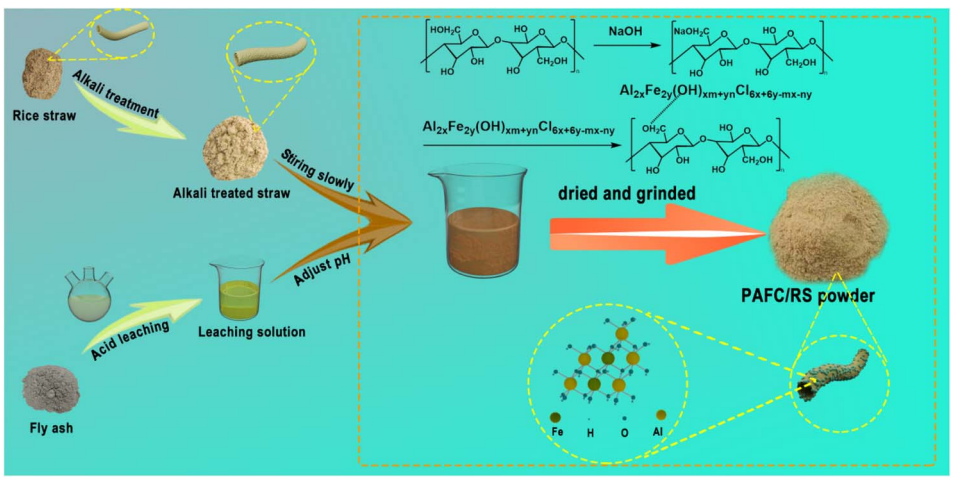

Fig. 1 Schematic for the preparation process of PAFC/RS.

$$3FeCl_3 + nH_2O \rightarrow Fe_2(OH)_nCl_{6-n}^{-} + nCl^{-} + nH^{+} \quad (1)$$

$$3AlCl_3 + mH_2O \rightarrow Al_2(OH)_mCl_{6-m}^{-} + mCl^{-} + mH^{+} \quad (2)$$

$$xAl_2(OH)_mCl_{6-m}^{-} + yFe_2(OH)_nCl_{6-n}^{-} \rightarrow Al_{2x}Fe_{2y}(OH)_{xm+yn}Cl_{6x+6y-mx-ny} \quad (3)$$

2.3. Structure characterization

X-ray diffraction (XRD) was used to analyze the phase of the sample (Ultima IV, Rigku, Japan) with a scan range of 2θ recorded from 20 to 80° at a scan speed of 2° per minute. The functional groups of the samples were analyzed with a Fourier transform infrared (FT-IR) spectrometer (Thermo IS10, Thermo Fisher Scientific, America). Topography of the sample was

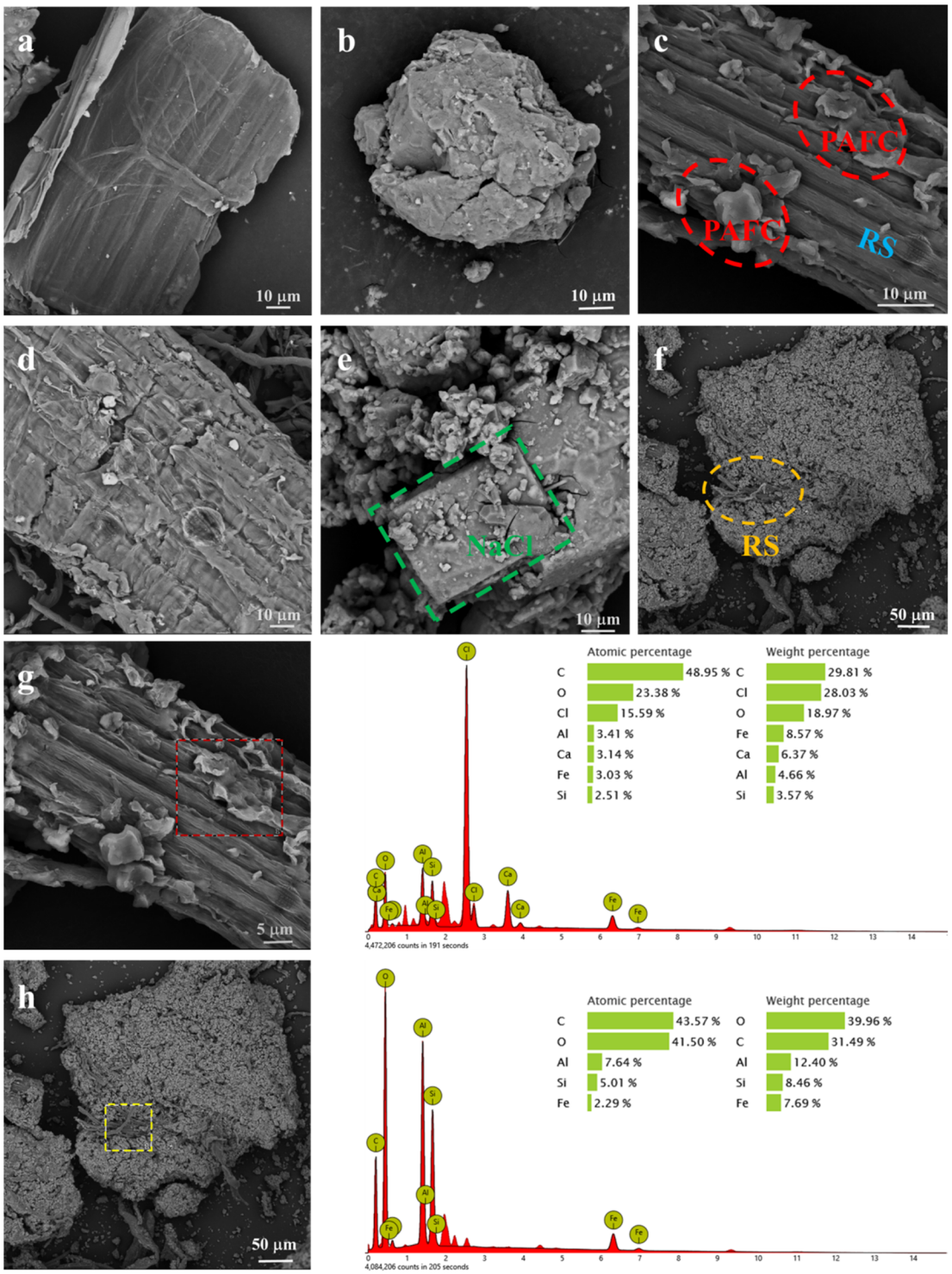

Fig. 2 The SEM pictures of (a) RS-0 (b) cPAFC (c) PAFC-10/RS-10 (d) RS-10 (e) PAFC (f) flocs and EDS images of (g) PAFC-10/RS-10 (h) flocs.

analyzed using a scanning electron microscope (SEM, Phenomenon LE). Inductively coupled plasma optical emission spectrometry (ICP-OES) (Optima8000, America) was used to quantify the residual metal ions in acid leaching solutions as well as treated water samples. Portable turbidimeter (Thermo Orion AQ3010) is used to test the turbidity of various water samples. Zeta potential tester (NANOZSE) was used to analyze the zeta potential of contaminant particles and flocs on the surface of raw wastewater and PAFC/RS treated wastewater.

2.4. Flocculation experiments

HA and kaolin were dissolved in deionized water to create a simulated coking wastewater solution. The pH of the simulated wastewater was adjusted using solutions of NaOH (10 wt%) or HCl (10%). Specifically, 0.1 g of NaOH and 0.25 g of HA were dissolved in deionized water to achieve a volume of 250 mL. A beaker containing 0.1 g of kaolin and 25 mL of aforementioned HA solution was stirred for 0.5 h. Then, deionized water was added to reaching a final volume of 500 mL to obtain a simulated wastewater with kaolin and HA concentrations of 200 and 50 mg L^{-1}, respectively.

Flocculants were added into 100 mL of simulated wastewater under magnetic stirring. The stirring process is divided into two stages: fast and slow stirring. In the first stage, the flocculant was rapidly mixed with the wastewater at 300 rpm for 1 min. Subsequently, a slower stirring speed of 50 rpm was maintained for 5 min. The stirring was then halted, to allow the solution to stand for 30 min. The upper clear liquid from the water surface was filtered and taken to measure the absorbance at 254 nm (UV_{254}) with a 1 cm diameter quartz colorimetric tube using a UV/visible spectrophotometer (MAPADA-1800pc-os2). COD test was according to the HJ 828-2017 standard.[14] Three parallel experiments were conducted for each sample, and the mean value was reported. In addition, flocs were filtered and dried to collect flocs for subsequent testing. COD, turbidity, and UV_{254} removal efficiency were all calculated according to eqn (4).

$$\text{Removal efficiency}(\%) = \frac{c_0 - c_1}{c_0} \times 100\% \quad (4)$$

where c_0 represents the initial concentration of COD, turbidity or UV_{254} in the wastewater before treatment, and c_1 represents the concentration of COD, turbidity or UV_{254} in the wastewater after treatment with PAFC/RS.

3. Results and discussion

3.1. Characterization of RS and RS-10

As an effective analytical technique, SEM can clearly show the morphology of materials. As shown in Fig. 2a, the surface of the non-alkali-treated straw is relatively smooth. In contrast, Fig. 2d reveals that the surface of RS-10 is rougher, providing a larger surface area. This facilitates the attachment of PAFC, resulting in a better composite of PAFC and RS-10.

The rice straw treated in aq. NaOH solutions for 24 h was analyzed using FTIR (Fig. 3 and S1†). The broad absorption peak at 3416 cm^{-1} signifies the stretching vibration of the –OH group. The peak at 1738 cm^{-1} is attributed to the stretching vibration of C=O. The adsorption peaks at 1247 cm^{-1} and 1511 cm^{-1} correspond to the C=C plane-symmetric stretching vibration of the aromatic ring found in lignin.[15] Compared to the spectrum of RS-0, RS-10 shows no absorption peaks at 1738 cm^{-1}, 1511 cm^{-1}, and 1247 cm^{-1}, indicating the removal of aromatic compounds and lignin from the straw.[13]

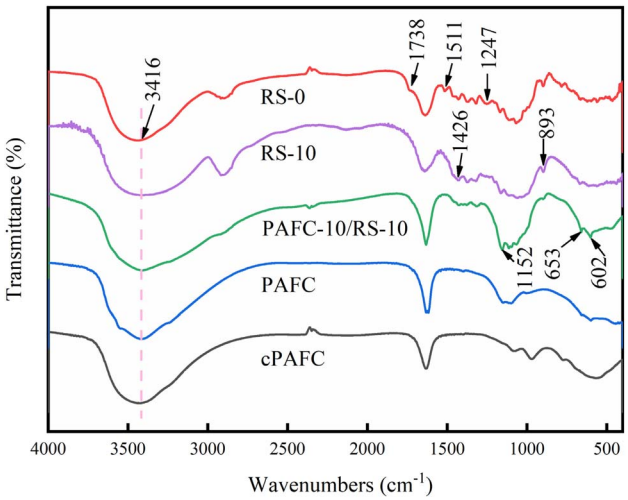

Fig. 3 FTIR spectra of RS-0, RS-10, PAFC-10/RS-10, PAFC, cPAFC.

3.2. Characterization of PAFC and PAFC-10/RS-10

3.2.1. FTIR. The effect of the chemical structure of PAFC-10/RS-10 on the flocculation properties was firstly studied by the FTIR spectroscopy. Fig. 3 shows an absorption peak at 1426 cm^{-1} in the RS-10 spectrum, attributed to cellulose. A broad absorption peak appears at the same position in the PAFC-10/RS-10 spectrum, indicating hydrogen bonding between PAFC and the hydroxyl groups of RS. Moreover, the small peak at 893 cm^{-1}, representing the deformation vibration of C–H and the bending vibration of –OH in the straw, is also observed in the spectrum of PAFC-10/RS-10. In the absorption

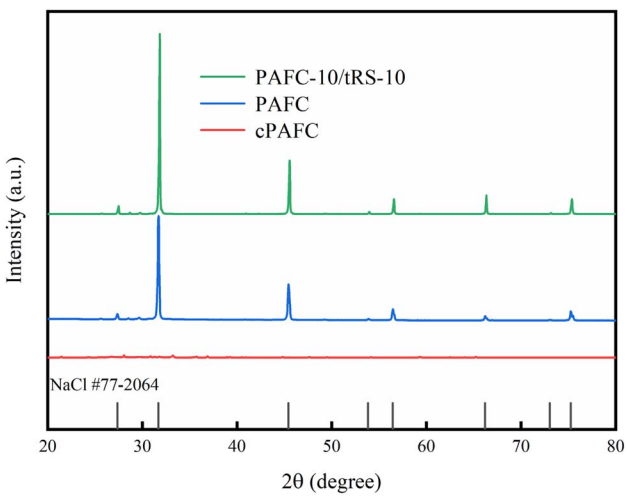

Fig. 4 XRD patterns of PAFC-10/RS-10, PAFC and cPAFC.

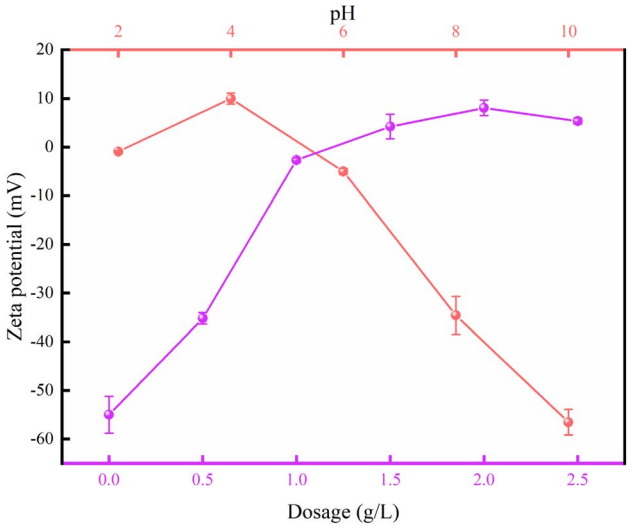

Fig. 5 Effect of flocculant dosage and pH on the surface charge of the flocs.

spectrum of PAFC-10/RS-10, the height of this peak was reduced due to hydrogen bonding between the hydroxyl groups in cellulose and PAFC, resulting in the weakening of –OH bending vibration.[11] However, absorption peaks at 1426 cm^{-1} and 893 cm^{-1} were not observed in the PAFC spectrum. The absorption peak at 1152 cm^{-1} in the spectra of PAFC and PAFC-10/RS-10 arises from the asymmetric stretching vibration of Fe–OH or Al–OH.[16] The absorption peaks at 653 cm^{-1} and 602 cm^{-1} in the infrared spectra of PAFC and PAFC-10/RS-10 are due to the spatial bending of Fe–OH and Al–OH.[12]

3.2.2. XRD. Fig. 4 displays the XRD patterns of various PAFC flocculants. Unlike the amorphous polymer cPAFC, the XRD patterns of PAFC and PAFC/RS show diffraction peaks of NaCl, but no diffraction peaks of $Fe(OH)_3$ and $Al(OH)_3$. This indicates that in addition to the formation of aluminum–iron based amorphous polymers, sodium chloride crystals were formed as a by-product. Importantly, Na^+ and Cl^- did not affect the flocculating efficiency of the flocculant.[17]

3.2.3. SEM and EDS. The morphology of the flocculants was examined by SEM, and EDS can provide information on the loading of PAFC on the RS. Fig. 2b shows cPAFC have rough surface and large size. While in Fig. 2e, alongside smaller-sized and smooth-surfaced PAFC, NaCl crystals are also observed, which is confirmed by the XRD spectra. Fig. 2c shows the microstructure of PAFC-10/RS-10, where the surface of RS presents distinct clumps. As shown in Fig. 2g, the selected area contains RS and clumps, which are rich in C, O, Al, and Fe. This indicates the successful loading of PAFC onto RS.

3.2.4. Zeta potential. In order to explore the flocculation ability of the flocculants, the surface potential of the pollutant particles and floc in the coking water was detected. As shown in Fig. 5, the zeta potential of the floc surface changed from −55.2 mV to 5.2 mV with increasing flocculant dosage. This is because the interaction of the HA in the wastewater with the flocculant causes the surface charge of the floc to be reversed.[18] When the amount of flocculant is 1 g L^{-1}, the surface potential of the flocs is close to 0. When the surface charge of the pollutant is neutralized, the colloidal solution beyond the stability point will destabilize, leading to flocculation and settling. The effectiveness of the flocculant decreases with increasing pH, consistent with results reported in the literature.[19] The flocculant has the best flocculation effect under weakly acidic conditions. The zeta potential results demonstrate that the optimal amount of flocculant and the appropriate pH are crucial for maximizing flocculant effectiveness.

3.3. Influential factors of simulated coking wastewater treatment performance

3.3.1. Actual flocculation effects and influencing factors. In Fig. 6a–d, the wastewater treated with PAFC-10/RS-10 exhibits

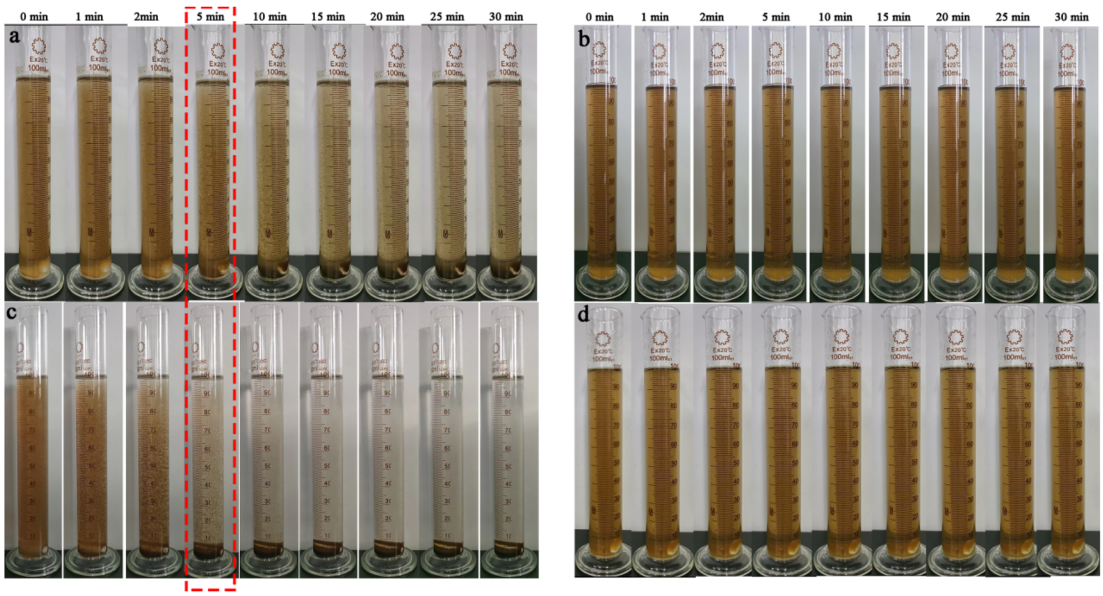

Fig. 6 The real-time images of the flocculation effect of (a) PAFC (b) raw (c) PAFC-10/RS-10 wastewater (d) RS.

the highest transparency among the four water samples. The flocs in the wastewater begin to settle significantly by the fifth minute, indicating that the flocculation effect of PAFC-10/RS-10 is superior to that of PAFC alone.

The relationship between dosage and flocculation performance was explored. The initial COD content and turbidity are 147 mg L^{-1} and 241.7 NTU, respectively. As shown in Fig. 7a, the COD removal efficiency increased and then decreased with the increase in PAFC-10/RS-10 dosage. Correspondingly, Fig. 7c shows that the turbidity removal rate of the wastewater increases with increasing dosage, reaches a peak, and then decreases, yet still maintains a high removal rate. The COD removal efficiency and turbidity removal efficiency are only 13.6% and 64.3%, respectively, when the PAFC-10/RS-10 dosage is 0.5 g L^{-1}. The highest COD removal of 79.7% (the COD value of the treated wastewater is 39.5 mg L^{-1}) and the highest turbidity removal of 97.3% (the turbidity is 6.5 NTU) were obtained at a dosage of 1 g L^{-1}. However, as the dosage of PAFC-10/RS-10 increased further, the COD removal rate decreased, and the turbidity removal rate, although still high, also showed a decline trend. Fig. S3 and S4† shows that the COD removal efficiency decreased from 79.1% to 48.5% with the addition of PAFC-10/RS-10 increased from 1 g L^{-1} to 2 g L^{-1}. This phenomenon indicated that excessive addition of PAFC-10/RS-10 not only failed to promote flocculation but also disrupted it. In conjunction with Fig. 5, it is observed that the charge on the surface of the flocculated clusters changes from negative to positive with increasing PAFC-10/RS-10 dosage. This is because the addition of too much flocculant will cause the potential of HA to reverse and reach a new equilibrium, resulting in poor flocculation. This is mainly due to the fact that the flocculation process initiated by PAFC-10/RS-10 is predominantly operated

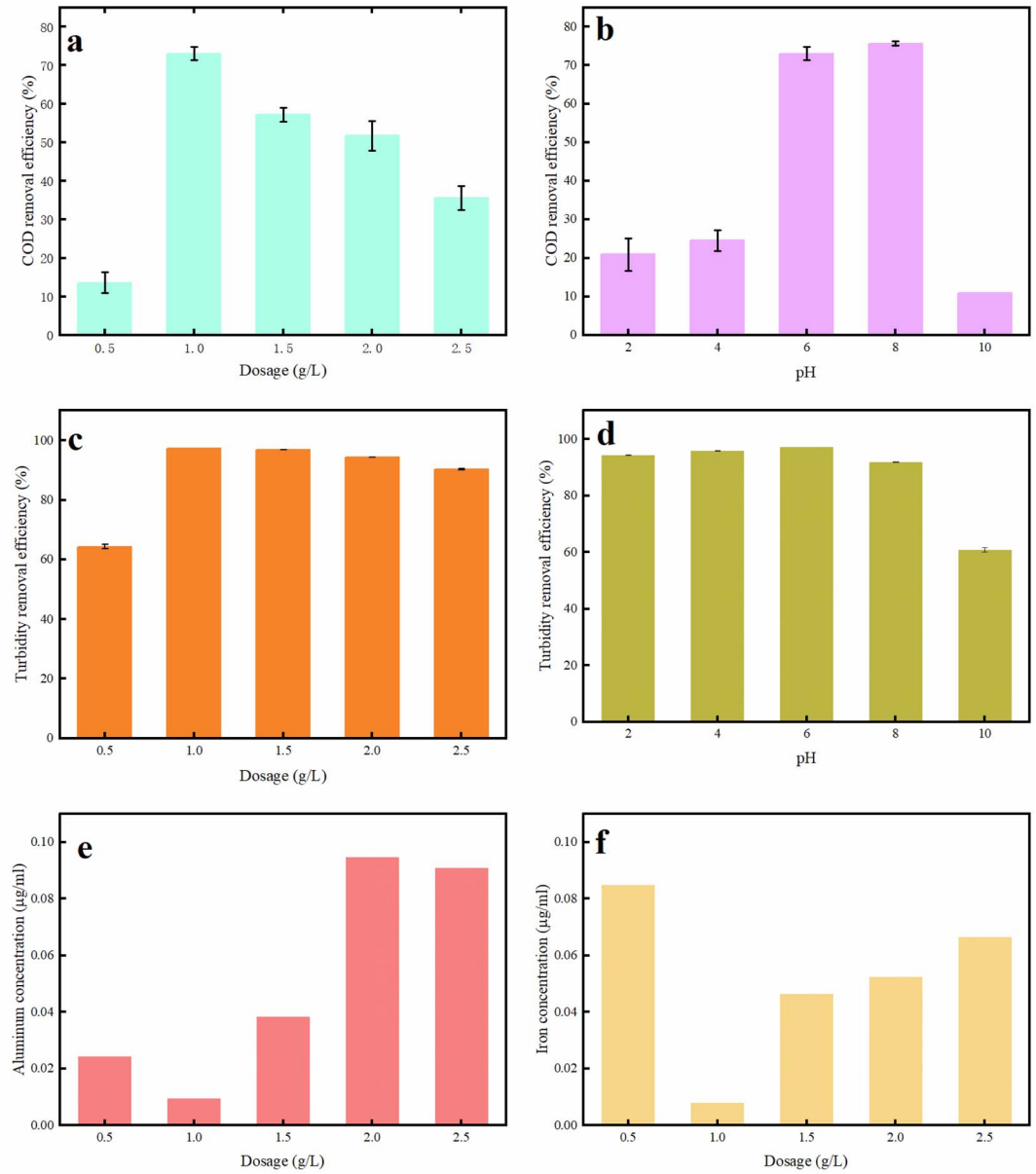

Fig. 7 Effect of (a) dosage (b) pH on flocculation, effect of (c) dosage (d) pH on turbidity, residual (e) aluminum and (f) iron in treated wastewater.

through two mechanisms: charge neutralization and adsorption bridging. Regarding charge neutralization, the suitable quantity of PAFC-10/RS-10 effectively neutralized the charge on the surface of colloidal particles in wastewater. That disrupted the charge balance and induced the sedimentation of colloidal particles. However, when an excessive amount of PAFC-10/RS-10 is added, the surface of some colloidal particles in the unstable wastewater system will carry the same charge as the flocculant.[20,21] Thus, the whole wastewater system will reach a stable state again, which resulted in halted sedimentation. Ultimately, removal efficiency of COD and turbidity in the wastewater did not increase with an increase in flocculant dosage, it may even decrease. Additionally, when considering the adsorption bridging mechanism, the excessive addition of flocculant leads to a mismatch between the number of colloidal particles and the elongated flocculant chain.[19] Furthermore, the quantity of colloidal particles in the wastewater is too small due to the excessive long chain of flocculant. Consequently, the elongated chain of colloidal particles remains unconnected to the exterior, resulting in insufficient stability of flocculation and reduced efficiency in wastewater treatment. In essence, there exists an optimal dosage for maximizing the efficiency of PAFC/RS in wastewater. For the simulated wastewater, it has been determined that a PAFC/RS dosage of 1 g L^{-1} not only yielded a relatively excellent flocculation effect but also contributed to a reduction in flocculation costs.

Fig. 7b and d illustrate that when the pH is below 6, the flocculant exhibits reduced removal efficiency for COD (below 30%), turbidity (below 95%) in the wastewater. The flocculant achieved optimal treatment efficacy when applied to simulated wastewater with an initial pH of approximately 7. At a pH of 10, the flocculant experienced complete failure, with the removal efficiency for COD significantly reduced to 10.9% and the turbidity removal rate reduced to 60.8%. This phenomenon is attributed to the abundance of H^+ ions at low pH levels, which inhibits the formation of the active components of the flocculant. This observation is consistent with previously reported findings.[22] Consequently, the flocculation ability of the flocculant is weakened. At pH levels of 8 or higher, the substantial presence of OH^- ions readily causes the flocculant to precipitate, resulting in a loss of its flocculation efficacy. At a pH of approximately 7, the flocculants exhibit a relatively high content of positive ions and hydrolyzed complexes.[23] During this phase, the charge neutralization and sweeping flocculation mechanisms facilitated the rapid complexation of HA molecules with positive ions and the bridging with hydrolyzed complexes.[18,19] Ultimately, rapid sedimentation of HA pollutants in wastewater was achieved. In summary, the optimal flocculation conditions were found to be an addition amount of 1 g L^{-1} and a pH range of 6–8. Moreover, Fig. 7e and f show that the concentration of aluminum (Al) in the treated wastewater was below 0.09 mg L^{-1}, meeting the permissible concentration for aluminum in drinking water, which is 2 mg L^{-1}.

3.3.2. Comparison with similar products. Table 1 compares the removal efficiencies of various flocculants for wastewater pollutants under their respective optimal flocculation conditions. The PAFC-10/RS-10 demonstrates an advantage over several inorganic flocculants of similar type. Researchers reported that a PAFC, after 90 min of flocculation, could achieve removal rates of 72.2% for COD and 79.2% for UV_{254}, respectively.[25] Furthermore, commercially available PAFC exhibited removal efficiencies of 63.2% for COD, 81.5% for UV_{254}, and 85.4% for turbidity, whereas PAFC-10/RS-10 demonstrated higher effectiveness with removal efficiencies of 79.7%, 98.2%, and 97.3% for COD, UV_{254} (Fig. S2†) and turbidity, respectively. Overall, the PAFC-10/RS-10 shows promising prospects for application in wastewater flocculation and purification.

3.4. Analysis of flocs

To understand the role of PAFC-10/RS-10 in the flocculation process, flocs collected from treated wastewater were characterized. As shown in Fig. 2f, the morphology of flocs from PAFC-10/RS-10 treated wastewater reveals that numerous small-sized particles are attached to the surface of the RS, and many flocs

Table 1 Comparison of the flocculation effect of several inorganic flocculants on wastewater[a]

Samples	Water resource	Stir rate (rapidly slowly)	Mixing time (rapidly slowly)	Setting time	pH	Dosage (mg L^{-1})	COD removal efficiency (%)	UV_{254} removal efficiency (%)	Colour (%)	Turbidity (%)	Ref
PAFCS	Coking water	200 rpm 80 rpm	1 min 15 min	15 min	9	300	44	47	—	93.32	24
PAFC	Landfill leachate	500 rpm 150 rpm	2 min 1 min	90 min	6	1200	72.2	79.2	82.9	—	25
$FeCl_3$	Landfill leachate	—	—	—	5.5	1000	89.0	—	—	—	26
PFSiC	Coking water	200 rpm 40 rpm	1 min 10 min	30 min	7.8	100	—	50.1	75.3	—	27
PAFSiC	Coking water	200 rpm 40 rpm	1 min 10 min	30 min	7.8	100	—	59.9	83.8	—	27
PAFC/RS	Coking water	300 rpm 80 rpm	1 min 5 min	30 min	7	1000	79.7	98.2	—	97.3	This work
cPAFC	Coking water	300 rpm 80 rpm	1 min 5 min	30 min	7	1000	63.2	81.5		85.4	This work

[a] COD: chemical oxygen demand; PAFC: polyaluminium ferric chloride; PFSiC: poly-ferric-silicate-chloride, PAFSiC: poly-aluminum-ferric-silicate-chloride, $FeCl_3$: ferric chloride.

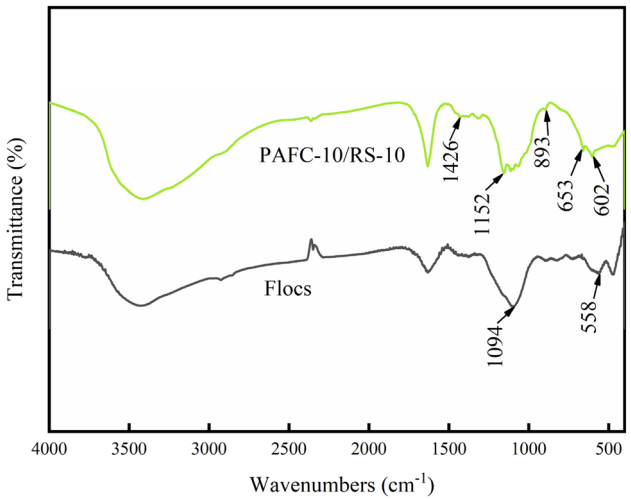

Fig. 8 The absorption spectra of the flocs and PAFC-10/RS-10.

are attached to one end of the RS. This indicates that the PAFC-loaded RS can aggregate flocculant particles and form large-sized flocs during the flocculation process. In Fig. 2h, the EDS plots of the flocs show high concentrations of C, O, Al, Fe, and Si elements in the selected area, indicating that the particulate matter encapsulating the RS is HA.

In Fig. 8 the absorption spectra of the flocs, the asymmetric stretching vibrational absorption peaks of Fe–OH or Al–OH were found to be blueshifted from 1152 cm^{-1} to 1094 cm^{-1}, suggesting that PAFC is involved in flocculation.[17] The peak at 1426 cm^{-1} which attributed to cellulose not be observed in spectra of flocs. The absorption peaks at 653 cm^{-1} and 602 cm^{-1} in the infrared spectra of PAFC-10/RS-10 are due to the bending vibrations of Fe–OH and Al–OH. However, the absorption peaks due to the bending vibrations of Fe–OH and Al–OH were shifted to 558 cm^{-1} in the absorption spectra of the flocculants, indicating the presence of hydrogen bonding between Fe–OH, Al–OH, and HA molecules.

4. Flocculation mechanism

The flocculation mechanism of the prepared PAFC-10/RS-10 on simulated coking wastewater is illustrated in Fig. 9. Negatively charged humic acid (HA) adsorbed onto the surface of kaolin particles forms a stable colloidal solution. As show in Fig. 9a, upon addition of PAFC-10/RS-10 to the wastewater, the negatively charged contaminant molecules interact with the positively charged polynuclear hydroxyl complex (PHC) flocculant in the solution. This interaction neutralizes the surface charge of pollutant particles, destabilizing their colloidal state.[28] Subsequently, from Fig. 9b, these destabilized particles accumulate on the surface of PAFC-10/RS-10, promoting a gradual increase in flocculant volume and accelerating settling. Additionally, certain dimers and trimers in the flocculants not only adsorb pollutant particles but also act as bridges for smaller flocs.[29] Over time, these colloidal particles fuse into larger flocs, further accelerating the settling process (Fig. 9c). During this complex process, some free-state pollutant colloidal particles and small flocs become encapsulated within larger flocs.[24] This process increases floc volume, removes pollutants, and forms a dense sediment layer. During flocculation, the unique rough surface of RS-10 serves a dual function: it provides a larger surface area for PAFC loading and enhances the efficacy of the flocculant in adsorbing colloidal particles and flocs, promoting rapid aggregation.

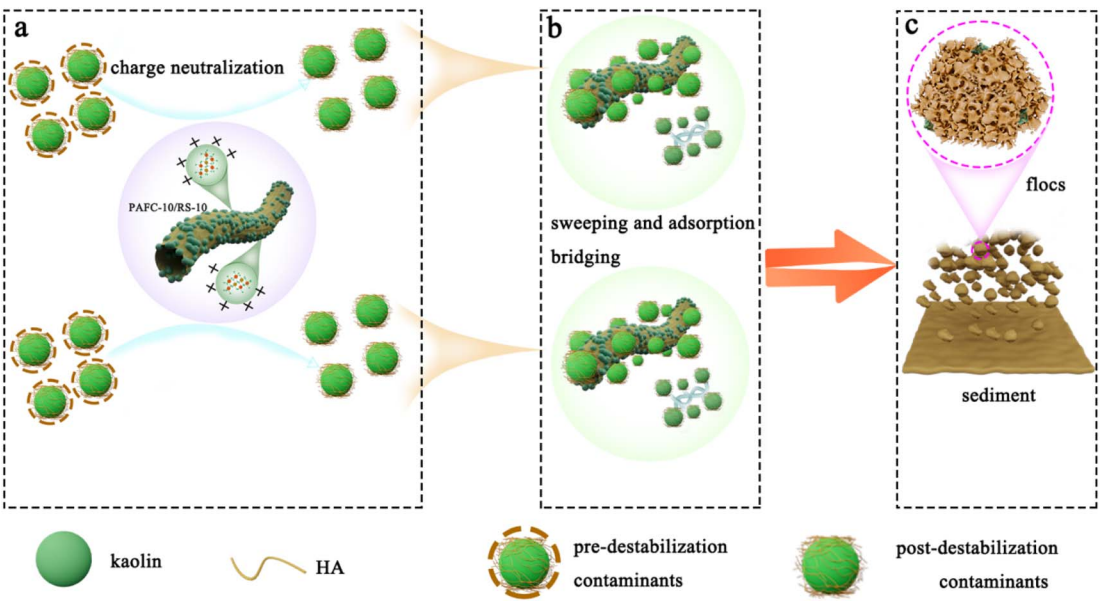

Fig. 9 Potential flocculation mechanism of PAFC/RS in the treatment of coking wastewater: (a) charge neutralization (b) sweeping and adsorption bridging (c) floc settlement.

5. Conclusions

In this study, PAFC/RS was prepared utilizing the acid leachate of fly ash and alkali-treated rice straw, showcasing a significant flocculation effect on the biochemical effluent of coking wastewater. Explored the influence of both preparation and flocculation conditions on the overall flocculation performance. Flocculation indices, comprising COD, UV_{254}, and residual Al in the treated wastewater, were assessed. The removal rates of turbidity, COD, and UV_{254} in PAFC/RS-treated wastewater attained 97.3%, 79.7%, and 98.2%, respectively, with a flocculant dosage of 1 g L^{-1} and a wastewater pH of 6–8. Experimental results confirmed that the inclusion of an appropriate amount of modified straw substantially improved the flocculation efficiency of PAFC. We investigated potential flocculation mechanisms of PAFC/RS, encompassing charge neutralization, adsorption bridging, and enhanced sweep flocculation. Although the composite flocculant prepared in this experiment still has limitations, such as high environmental requirements and a narrow range of wastewater types it can treat, these shortcomings do not overshadow the advantages in terms of cost and flocculation efficiency demonstrated by the composite flocculant developed in this study. In conclusion, this study adeptly integrated fly ash and straw to explore a cost-effective method for producing a water treatment agent. These findings are expected to provide valuable insights into wastewater flocculation treatment.

Data availability

The authors confirm that the data supporting the findings of this study are available within the article [and/or its ESI†].

Conflicts of interest

The authors declare that they have no known competing financial interests or personal relationships that could have appeared to influence the work reported in this paper.

Acknowledgements

We are grateful for the financial support of this research from National Key Research and Development Project (2019YFC1908204), Guiding projects in Fujian Province (2023H0023), Fuzhou Science and Technology Plan Project (2022-P-012).

References

1 J. Wang, S. Wang and C. Hu, *Chemosphere*, 2024, **349**, 140923.
2 J. Li, X. Yuan, H. Zhao, F. Li, Z. Lei and Z. Zhang, *Bioresour. Technol.*, 2018, **247**, 1206.
3 M. Zheng, N. Zhou, S. Liu, C. Dang, Y. Liu, S. He, Y. Zhao, W. Liu and X. Wang, *J. Cleaner Prod.*, 2019, **213**, 365.
4 M. Liu, S. Preis, I. Kornev, Y. Hu and C. H. Wei, *J. Environ. Sci.*, 2018, **64**, 306.
5 J. Wang, F. Chang and M. Zheng, *Int. J. Environ. Res. Public Health*, 2023, **20**, 6342.
6 X. Xia, S. Lan, X. Li, Y. Xie, Y. Liang, P. Yan, Z. Chen and Y. Xing, *Chemosphere*, 2018, **206**, 701–708.
7 V. Ajao, H. Bruning, H. Rijnaarts and H. Temmink, *Chem. Eng. J.*, 2018, **349**, 622–632.
8 P. F. Sun, H. Lin, G. Wang, L. L. Lu and Y. H. Zhao, *J. Hazard. Mater.*, 2015, **284**, 215–221.
9 M. Wang, L. Feng, X. You and H. Zheng, *Chemosphere*, 2021, **264**, 128525.
10 R. Koshani, M. Tavakolian and T. G. M. van de Ven, *J. Mater. Chem. B*, 2020, **8**, 10502.
11 A. G. Souza, D. F. Santos, R. R. Ferreira, V. Z. Pinto and D. S. Rosa, *Int. J. Biol. Macromol.*, 2020, **165**, 1803.
12 X. Liu, Z. Wu, Y. Han and L. Han, *Energy*, 2017, **133**, 299.
13 J. Wang, Y. Zuo, J. Xiao, P. Li and Y. Wu, *Constr. Build. Mater.*, 2019, **228**, 116712.
14 P. Xu, H. Han, H. Zhuang, B. Hou, S. Jia, C. Xu and D. Wang, *Bioresour. Technol.*, 2015, **182**, 389.
15 H. Ren, Z. Xu, C. Du, Z. Ling, W. Yang, L. Pan, Y. Tian, W. Fan and Y. Zheng, *Int. J. Biol. Macromol.*, 2023, **242**, 124938.
16 X. Wang, C. Shi, X. Hao, M. C. M. van Loosdrecht and Y. Wu, *Water Res.*, 2023, **231**, 119658.
17 Y. Chen, Y. Matsui, T. Sato, N. Shirasaki and T. Matsushita, *Water Res.*, 2023, **235**, 119909.
18 J. L. Lin, C. Huang, B. Dempsey and J. Y. Hu, *Water Res.*, 2014, **56**, 314.
19 Z. L. Yang, B. Y. Gao, Q. Y. Yue and Y. Wang, *J. Hazard. Mater.*, 2010, **178**, 596.
20 C. Shi, Q. Wang, D. Li, B. Zeng, Q. Liu, Y. Cui, J. Wang and X. Wang, *Sep. Purif. Technol.*, 2023, **313**, 123482.
21 V. H. Lim, Y. Yamashita, K. Ogawa and Y. Adachi, *J. Environ. Chem. Eng.*, 2021, **9**, 106481.
22 N. Shirasaki, T. Matsushita, Y. Matsui, A. Oshiba, T. Marubayashi and S. Sato, *Water Res.*, 2014, **48**, 375–386.
23 R. Jiao, R. Fabris, C. W. K. Chow, M. Drikas, J. van Leeuwen and D. Wang, *Chemosphere*, 2016, **150**, 211.
24 J.-M. Gao, B. Wang, W. Li, L. Cui, Y. Guo and F. Cheng, *Sep. Purif. Technol.*, 2023, **306**, 122545.
25 Y. Cheng, L. Xu and C. Liu, *Environ. Technol. Innovation*, 2022, **27**, 102509.
26 B. K. Tripathy and M. Kumar, *Waste Manage.*, 2019, **85**, 18.
27 J. Li, X. Liu and F. Cheng, *Chem. Eng. J.*, 2017, **324**, 10.
28 Y. Xue, Z. Liu, A. Li and H. Yang, *J. Environ. Sci.*, 2019, **81**, 168.
29 Z. Liu, M. Huang, A. Li and H. Yang, *Water Res.*, 2017, **119**, 57.